Research Article

In Silico Study of Flavonoid Compounds from *Syzygium cumini* as Antioxidants Targeting Calmodulin-Ca^{2+}

Neona Dwi Nila Cahyani[1], Lilik Maslachah[2*], Rimayanti[3], Kadek Rachmawati[2], Ratna Damayanti[2], Moh. Sukmanadi[2]

[1]Faculty of Veterinary Medicine, Universitas Airlangga, Surabaya, Indonesia; [2]Department of Basic Veterinary Science, Faculty of Veterinary Medicine, Universitas Airlangga, Surabaya, Indonesia; [3]Department of Veterinary Reproduction, Faculty of Veterinary Medicine, Universitas Airlangga, Surabaya, Indonesia.

Abstract | This study evaluated *Syzygium cumini* flavonoids (quercetin, myricetin, rutin, and kaempferol) targeting the calmodulin-Ca^{2+} complex using *in silico* molecular docking with Gnina software. Rutin displayed the lowest binding free energies (ΔG) of -8.45 and -8.23 kcal/mol across two distinct grid box areas, stabilized by hydrogen bonds with residues Arg90, Arg86, Glu82, Thr26, Asp24, and Thr62. Computational predictions using SwissADME, ProTox-II, and PASS Online were also evaluated. Pharmacokinetic analysis indicated that rutin violates four Lipinski parameters, restricting passive oral absorption. Toxicity screening classified rutin and kaempferol as Class 5, while quercetin and myricetin were classified as Class 3. Biological activity tests yielded antioxidant probability (Pa) values of 0.87, 0.92, 0.92, and 0.86 for quercetin, myricetin, rutin, and kaempferol, respectively. All compounds shared an identical probability of inactivity value (Pi = 0.003) due to the structural similarities of their core scaffolds within the database baseline. Overall, rutin demonstrates a structural baseline for the antioxidant regulation of Ca^{2+} homeostasis. However, this study functions as a preliminary screening, and these computational predictions require direct experimental validation.

Keywords | Antioxidants, Calmodulin-Ca^{2+}, Flavonoids, *In silico*, Molecular docking, *Syzygium cumini*

Received | May 17, 2026; **Accepted** | July 10, 2026; **Published** | August 08, 2026
***Correspondence** | Lilik Maslachah, Department of Basic Veterinary Science, Faculty of Veterinary Medicine, Universitas Airlangga, Surabaya, Indonesia; **Email:** lilik.maslachah@fkh.unair.ac.id
Citation | Cahyani NDN, Maslachah L, Rimayanti, Rachmawati K, Damayanti R, Sukmanadi M (2026). *In silico* study of flavonoid compounds from *Syzygium cumini* as antioxidants targeting calmodulin-Ca^{2+}. Adv. Anim. Vet. Sci., 14(8):1832-1844.
DOI | https://dx.doi.org/10.17582/journal.aavs/2026/14.8.1832.1844
ISSN (Online) | 2307-8316

INTRODUCTION

Syzygium cumini, a tropical tree species within the Myrtaceae family, is widely distributed throughout Southeast Asia, particularly in Indonesia. Beyond its utility as a food source, various botanical parts of this plant have been extensively employed in traditional medicine. The seeds of *S. cumini* are rich in diverse bioactive metabolites, including alkaloids, flavonoids, amino acids, glycosides, phytosterols, steroids, tannins, triterpenes, and saponins (Hidayah *et al*., 2023). The seeds and fruits of *S. cumini* serve as a concentrated natural source where these four specific flavonoids (quercetin, myricetin, rutin, and kaempferol) co-occur (Kumar *et al*., 2022). Among these, flavonoids serve as potent antioxidants by neutralizing free radicals, thereby safeguarding cellular integrity from oxidative stress-induced damage (Ontiveros *et al*., 2019).

Antioxidants are molecules that inhibit the oxidation of other molecules by preventing electron transfer. Excessive levels of reactive oxygen species (ROS) can disrupt the balance between oxidants and antioxidants, leading to oxidative stress and molecular damage (Munteanu and Apetrei, 2021). Flavonoids, particularly those found in *S.*

cumini fruit such as quercetin, exhibit strong antioxidant capacity and may act as non-competitive inhibitors in the regulation of calcium ions (Ca^{2+}), which play a significant role in cellular oxidative mechanisms (Ontiveros *et al*., 2019). Pharmacokinetic studies demonstrate that after dietary intake, typical plasma concentrations of quercetin and its metabolites reside within the nanomolar to low micromolar range, starting around 28-142 nM and reaching 0.3-0.75 µmol/l following flavonoid-rich meals (Manach *et al*., 1998; Spencer *et al*., 2008).

The interaction between Ca^{2+} and ROS has been widely documented, especially in the context of cardiovascular diseases, where it contributes to cellular injury associated with oxidative stress (Hempel and Trebak, 2017). Among the diverse calcium-regulated functions, cellular apoptosis and energy metabolism are particularly relevant to oxidative stress, as mitochondrial Ca^{2+} overload disrupts electron transport, increases ROS production, and triggers apoptotic cascades (de Nicolo *et al*., 2023; Giorgi *et al*., 2018; Bertero and Maack, 2018). A reciprocal relationship exists between Ca^{2+} and ROS in regulating intracellular calcium signaling, with Ca^{2+} also participating in ROS generation (de Nicolo *et al*., 2023).

One of the main proteins involved in calcium signaling and its interaction with ROS is calmodulin. Calmodulin is a multifunctional calcium-binding messenger protein that can bind up to four Ca^{2+} ions through four EF-hand domains located at its N- and C-terminal lobes, connected by a flexible central linker (Pepke *et al*., 2010). The 1CLL structure (Chattopadhyaya *et al*., 1992) was selected because it represents a high-resolution (1.7 Å) X-ray crystal structure of fully calcium-saturated mammalian calmodulin in its uncomplexed open conformation. This unliganded open state represents a widely used reference conformation for calmodulin-ligand docking studies due to its completeness, high resolution, and absence of bound exogenous ligands.

The proposed mechanism follows a sequential cascade: flavonoids bind to calmodulin at its calcium-binding domains, which inhibits calmodulin's ability to activate NADPH oxidase 5 (NOX5). NOX5 requires calmodulin for calcium-dependent superoxide production; thus, flavonoid-mediated inhibition of this interaction reduces NOX5 activity and downstream ROS generation. This sequence positions flavonoid-calmodulin binding as the primary upstream event that limits oxidative stress through enzymatic ROS suppression (Tirone and Cox, 2007; Millana-Fañanás *et al*., 2020; Sakurada *et al*., 2019). Additionally, flavonoids may alter the Ca^{2+} binding affinity of calmodulin or compete with calmodulin for binding to NOX, further diminishing ROS production (Sakurada *et al*., 2019). This mechanism is supported by prior studies showing that flavonoids like quercetin act as anticalmodulin agents to inhibit calmodulin-dependent enzymes (Paliyath and Poovaiah, 1985; Picq *et al*., 1989). More recent evidence confirms that flavonoids modulate calmodulin-dependent signaling at physiologically relevant concentrations. Quercetin inhibits calcium/calmodulin dependent protein kinase IV (CaMKIV) with IC50 values in the micromolar range (Gupta *et al*., 2020), while rutin activates the calmodulin-dependent protein kinase kinase β/AMPK (CaMKKβ/AMPK) pathway (Ma *et al*., 2022). These findings corroborate the established anticalmodulin activity of flavonoids and support their potential to modulate calmodulin-dependent enzymatic functions.

To further understand the interaction among flavonoids, Ca^{2+}, and calmodulin, an *in silico* approach provides an efficient and cost-effective method. Computer-based simulations enable virtual screening, ligand-based drug design, and prediction of biological activity, thereby accelerating the early phases of pharmaceutical research (Shaker *et al*., 2021). Based on the complex interplay among ROS, Ca^{2+}, and flavonoids, this study aims to explore the potential of flavonoid compounds from *Syzygium cumini* as antioxidants through an in silico approach. Specifically, the research focuses on the molecular mechanisms by which flavonoids may regulate Ca^{2+} ions and reduce oxidative stress by interacting with the calmodulin-Ca^{2+} complex. We hypothesize that specific flavonoids from *Syzygium cumini* can stably bind to calmodulin-Ca^{2+} complexes within physiological concentration thresholds, as predicted by their binding affinities and interaction patterns, thereby serving as structural candidates for further experimental validation.

MATERIALS AND METHODS

Receptor preparation

The crystal structure of calmodulin (PDB ID: 1CLL) was retrieved from the RCSB Protein Data Bank and verified for completeness, utilizing the structure in its native crystal conformation without external energy minimization to preserve its coordinates. Receptor preparation was performed using AutoDock Tools version 1.5.7, involving the complete removal of solvent water molecules and co-crystallized ligands while retaining essential structural Ca^{2+} ions. Two distinct grid box configurations were established to target specific physically separate functional calcium-binding sites. Grid 1 was parameterized with dimensions of 36 x 42 x 30 Å centered at (x: 15.167, y: 30.608, z: 10.946) to encompass the C-terminal Ca-3 binding domain cluster, while Grid 2 utilized localized dimensions of 12 x 12 x 12 Å centered at (x: 0.027, y: 48.422, z: 21.504) to target the coordinating regions of both the N-terminal Ca-1 and Ca-2 domains. The final processed receptor was exported

and maintained in standard .pdb format for direct input into the Gnina docking simulations.

Ligand preparation

The 3D structures of quercetin (CID: 5280343), myricetin (CID: 5281672), rutin (CID: 5280805), and kaempferol (CID: 5280863) were retrieved from the PubChem database in their native, uncharged neutral protonation states and standard lowest-energy native tautomeric forms to serve as a uniform comparative baseline across all test groups. The initial .sdf files containing pre-computed 3D conformations were converted into .pdb format using Discovery Studio Visualizer for compatibility with the docking simulations, omitting additional external force field minimization as the Gnina engine handles conformation sampling and geometry optimization internally during simulation runs.

Pharmacokinetic test

Drug-likeness profiles were evaluated using SwissADME based on Lipinski's Rule of Five criteria to analyze individual topochemical descriptors, including molecular weight, lipophilicity, and hydrogen-bonding capacity. SMILES strings for each ligand were utilized as input prior to subsequent toxicity screening. Users should note that SwissADME's topological algorithms heavily weight multiple free hydroxyl groups, which can result in lower calculated log P values for polyhydroxylated flavonoids compared to their true experimental benchmarks.

Toxicity test

Acute toxicity profiles were established using the ProTox-II platform. SMILES strings for each flavonoid were utilized to predict median lethal dose (LD_{50}) values and their corresponding toxicity classifications (Classes 1–6) across Classes 1–6 based on Globally Harmonized System (GHS) criteria.

Biological activity test

The biological activity spectra of the ligands were predicted using the PASS Online server. SMILES strings were utilized to estimate the probability of activity (Pa) values and probability of inactivity (Pi) values based on Multilevel Neighbors of Atoms (MNA) descriptors, with a specific focus on the antioxidant potential of the investigated flavonoids to evaluate structural probability trends across identical core scaffolds.

Molecular docking

Molecular docking simulations were executed using the Gnina engine via a cloud-based implementation. The scoring architecture utilized the default integrated empirical scoring function combined with a convolutional neural network (CNN) model to generate scoring outputs. For each ligand, nine binding poses were generated per individual docking run within each specified grid box region to ensure thorough conformational sampling. From these generated poses, the conformation exhibiting the lowest binding free energy (ΔG) was selected for subsequent visualization and interaction profiling. The default Gnina scoring function was applied with an exhaustiveness value of 8, focused within targeted coordinate volumes. All water molecules and co-crystallized non-amino acid ligands were removed prior to execution, retaining only the structural calcium ions to maintain a dehydrated, unliganded receptor environment. To ensure exact reproducibility, the simulations were driven by the following command execution: !./gnina -r 1CLL_pure.pdb -l [Ligand].pdb --center_x [x] --center_y [y] --center_z [z] --size_x [size_x] --size_y [size_y] --size_z [size_z] -o [Output].sdf --seed 0. For each run, exactly 9 conformational binding poses were generated per ligand from which the lowest energy pose was selected.

Visualization

Molecular interactions were visualized in 2D and 3D formats using Discovery Studio Visualizer. The most stable ligand–receptor conformations were analyzed to identify hydrogen bonds, hydrophobic contacts, and electrostatic forces. Interatomic distances (Å) were measured between ligand atoms and specific coordinating residues. Additionally, 3D surface mapping was performed to verify the spatial orientation and positioning of the flavonoids within the calmodulin binding pockets.

Data analysis

Data analysis was conducted based on the minimum binding free energy (ΔG) scores from a single optimization routine. The 9 generated poses reflect distinct geometric conformations from a single search algorithm rather than independent statistical replicates; thus, the pose with the lowest absolute ΔG value was isolated. Lower ΔG values indicate stronger binding affinity; therefore, compounds exhibiting the most negative binding free energy (ΔG) values are interpreted to possess the highest thermodynamic stability and energetically favorable binding affinity within the target sites. Additionally, molecular interaction visualization, pharmacokinetics, toxicity, and predicted biological activities were evaluated to support the interpretation of results.

RESULTS

Pharmacokinetic test

Pharmacokinetic evaluation via SwissADME revealed the drug-likeness profiles of the four flavonoids based on Lipinski's Rule of Five. Pharmacokinetic parameters for all evaluated compounds are summarized in Table 1. Quercetin,

myricetin, and kaempferol displayed molecular weights (MW) of 302.24, 318.24, and 286.24 g/mol, with Log P values of -0.56, -1.08, and -0.03, respectively, denoting a hydrophilic character within permissible physiological thresholds for baseline absorption. These ligands featured 4–6 hydrogen-bond donors and 6–8 acceptors, with molar refractivity ranging from 76.01 to 80.06 cm^3/mol. These topochemical estimations differ from reported experimental literature values (approximately 1.82 for quercetin, 2.94 for myricetin, and 3.11 for kaempferol), revealing a localized hydrophilic bias in the software's fragmental calculations for heavily polyhydroxylated structures. In contrast, rutin violated four separate Lipinski criteria, exhibiting a MW of 610.52 g/mol, 10 donors, 16 acceptors, and a molar refractivity of 141.38 cm^3/mol. The server-generated Log P value of -3.89 differs from the experimental literature baseline of -2.11 (Guedes *et al*., 2026). Due to these extensive violations predicting poor oral bioavailability, rutin's practical relevance is directed toward alternative delivery frameworks, such as nanoparticle formulations or non-oral administration routes, rather than standard oral delivery.

Table 1: Results of pharmacokinetic test on quercetin, myricetin, rutin, and kaempferol.

Ligand	Molecular weight (g/mol)	Log p	Hydrogen bond donors	Hydrogen bond acceptors	Molar refractivity (cm^3/mol)
Quercetin	302.24	-0.56	5	7	78.03
Myricetin	318.24	-1.08	6	8	80.06
Rutin	610.52	-3.89	10	16	141.38
Kaempferol	286.24	-0.03	4	6	76.01

Toxicity test

Toxicity profiles predicted via ProTox II revealed distinct safety levels among the investigated flavonoids (Table 2). Quercetin and myricetin were categorized under toxicity class 3, both exhibiting an LD_{50} value of 159 mg/kg. This computational prediction for quercetin closely mirrors experimental rodent data, which reports acute oral LD50 values of 161 mg/kg for rats and 159 mg/kg for mice (Chang *et al*., 2021), confirming the baseline reliability of the predictive model. Conversely, kaempferol and rutin demonstrated lower predicted acute toxicity, falling into class 5 with exact server-generated LD50 values of 3919 mg/kg and 5000 mg/kg, respectively. These results indicate that rutin and kaempferol possess a lower toxicity profile within the calculated baseline. The server-generated point metrics represent acute threshold values derived from deterministic fragment similarity libraries without probabilistic variance measurements.

Biological activity test

PASS online analysis evaluated the antioxidant potential of the ligands based on structural probability scores (Table 3). Myricetin and rutin displayed comparable activity values at 0.924 and 0.923, respectively, followed by quercetin (0.872) and kaempferol (0.856). In this predictive framework, a Pa score above 0.7 indicates a high probability of exhibiting the targeted activity in experimental settings rather than an absolute certainty. This calculated probability matches documented in vitro antioxidant capacities for these specific chemical structures, though assay-dependent variations are acknowledged (Tessema *et al*., 2023). Each compound yielded an identical raw Pi value of 0.003. This uniform output reflects the close structural similarity of the polyhydroxylated flavonol cores within the software's training baseline database, rather than manual rounding.

Table 2: Predicted toxicity values of quercetin, myricetin, rutin, and kaempferol.

Ligand	LD_{50} (mg/kg)	Predicted toxicity class
Quercetin	159	3
Myricetin	159	3
Rutin	5000	5
Kaempferol	3919	5

Table 3: Pa and Pi values for antioxidant activity of quercetin, myricetin, rutin, and kaempferol.

Ligand	Pa	Pi
Quercetin	0.872	0.003
Myricetin	0.924	0.003
Rutin	0.923	0.003
Kaempferol	0.856	0.003

Table 4: Binding free energies (ΔG) of flavonoid ligands in the first and second grid box areas.

Ligand	The lowest ΔG value (kcal/mol)	
	First grid box area	Second grid box area
Quercetin	-6.82	-6.18
Myricetin	-7.18	-4.42
Rutin	-8.45	-8.23
Kaempferol	-6.92	-4.02

Molecular docking

Molecular docking simulations were executed using the Gnina engine with a fixed random seed parameter (--seed 0) to ensure strict algorithmic determinism and exact point estimate reproducibility. Rutin yielded the lowest binding free energies (ΔG) of -8.45 kcal/mol in the first grid box area and -8.23 kcal/mol in the second region (Table 4). Within the first grid box space (targeting the Ca-3 binding site cluster), the affinity followed the order of myricetin (-7.18 kcal/mol), kaempferol (-6.92 kcal/mol), and quercetin (-6.82 kcal/mol). Conversely, in the second grid box region (targeting the separate Ca-1 and Ca-2 binding

domains), the rank order shifted, with quercetin displaying lower binding energy (-6.18 kcal/mol) than myricetin (-4.42 kcal/mol) and kaempferol (-4.02 kcal/mol). This variation is due to the differing amino acid topologies between the two distinct search spaces, as visually mapped in Figures 1 and 2, where differences within 0.1 kcal/mol sit within the intrinsic scoring error margin. Calmodulin was selected as the target receptor due to its role as a cellular calcium sensor that maintains a direct regulatory feedback loop with intracellular reactive oxygen species (ROS) production, providing a baseline structural screening to address the lack of direct experimental binding data for these compounds in existing literature.

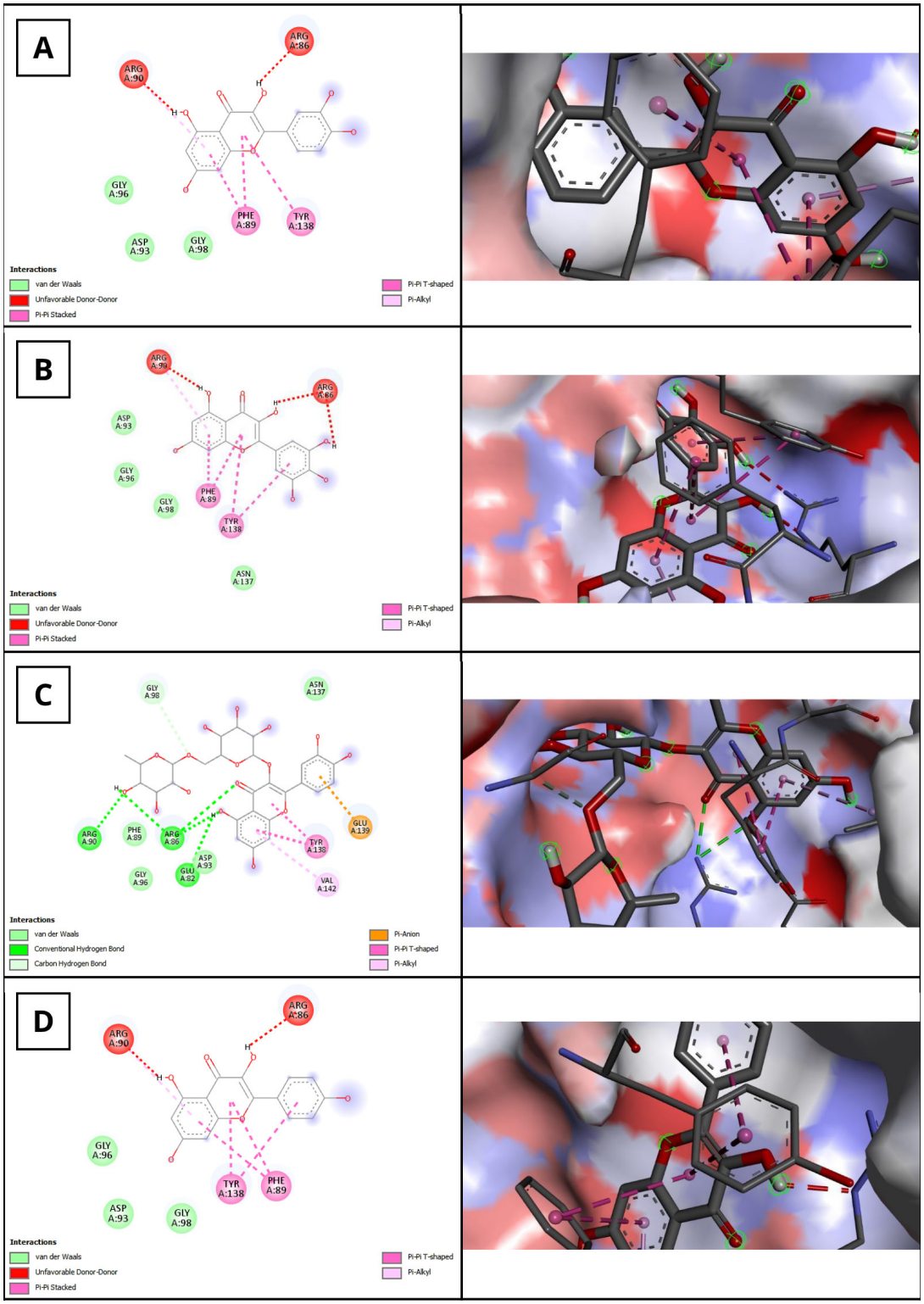

Figure 1: 2D and 3D visualizations of ligand–receptor interactions in the first grid box area. A: Quercetin; B: Myricetin; C: Rutin; D: Kaempferol. Interaction line codes are defined in the embedded figure legends, and 3D ribbon colors follow the standard sequence spectrum.

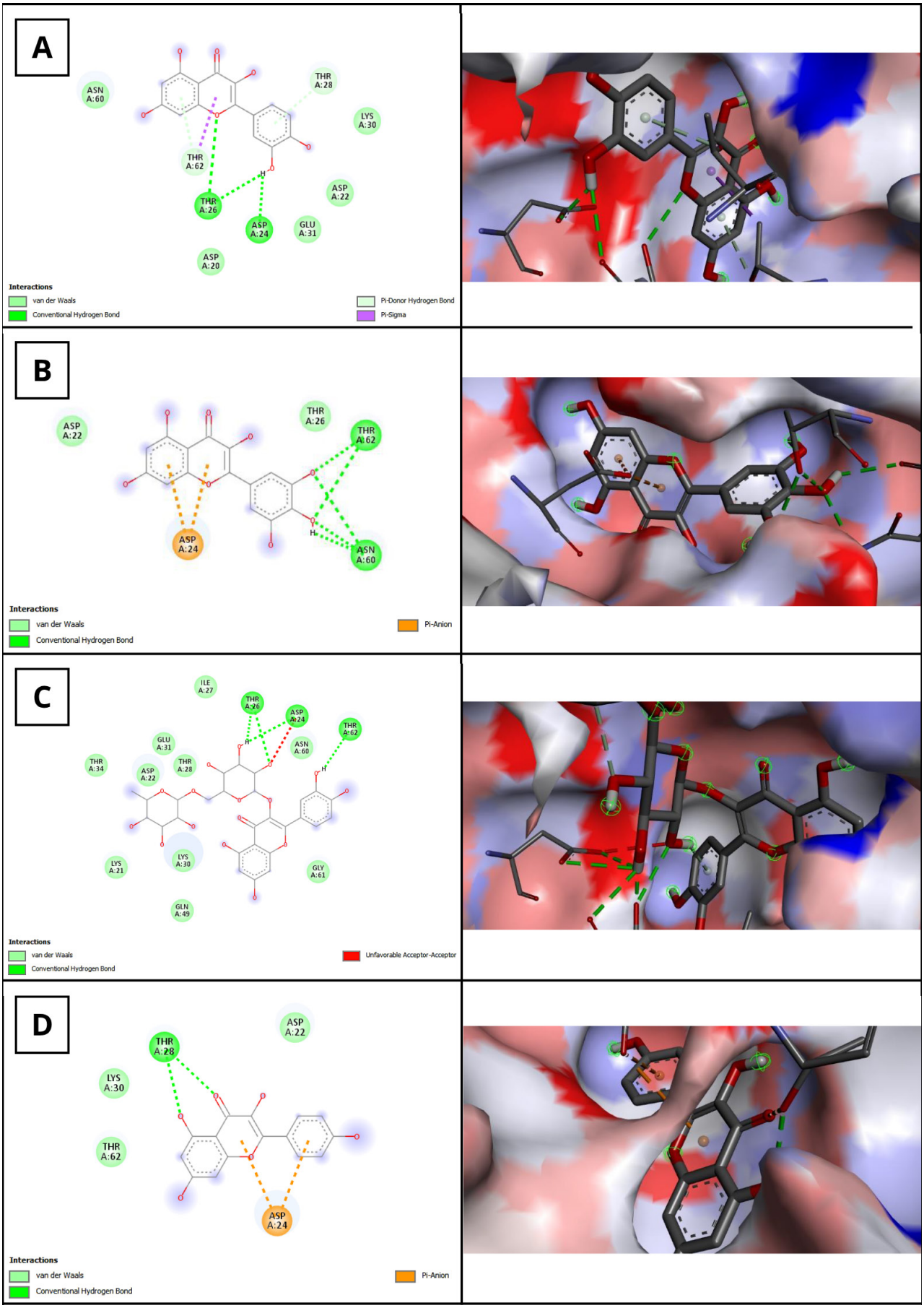

Figure 2: 2D and 3D visualizations of ligand–receptor interactions in the second grid box area. A: Quercetin; B: Myricetin; C: Rutin; D: Kaempferol. Interaction line codes are defined in the embedded figure legends, and 3D ribbon colors follow the standard sequence spectrum.

Table 5: 2D interaction analysis between ligands and the receptor in the first and second grid box areas.

Ligand	ΔG value (kcal/mol)	Hydrogen bonds		Hydrophobic interactions	Electrostatic interactions
		Amino acid	Distance (Å)		
First grid box area (Ca-3 binding site)					
Quercetin	-6.82	-	-	Gly96, Asp93, Gly98, Phe89, Tyr138	-
Myricetin	-7.18	-	-	Asp93, Gly96, Gly98, Asn137, Phe89, Tyr138	-
Rutin	-8.45	Arg90 Arg86 Glu82 Gly98	2.81 2.17 2.74 3.76	Phe89, Gly96, Asp93, Asn137, Tyr138, Val142	Glu139
Kaempferol	-6.92	-	-	Tyr138, Phe89, Gly96, Asp93, Gly98	-
Second grid box area (Ca-1 & Ca-2 Binding Sites)					
Quercetin	-6.18	Thr26 Asp24 Thr62 Thr28	2.78 2.15 3.60 3.31	Asn60, Asp20, Glu31, Asp22, Lys30	-
Myricetin	-4.42	Asn60 Thr62	2.49 2.94	Thr26, Asp22	Asp24
Rutin	-8.23	Thr26 Asp24 Thr62	1.74 2.76 2.17	Thr34, Lys21, Asp22, Lys30, Glu31, Thr28, Ile27, Asn60, Gly61, Gln49	-
Kaempferol	-4.02	Thr28	2.70	Asp22, Lys30, Thr62	Asp24

Note: Highlighted residues indicate specific binding sites: yellow (Ca-3), blue (Ca-1), and green (Ca-2) (Chattopadhyaya *et al.*, 1992).

Visualization

Residue-level interaction mapping via Discovery Studio Visualizer identified binding residues across both grid regions and is compiled by individual grid box sections in Table 5. In the first grid, which focused on the third calcium-binding domain (Ca-3), rutin generated the lowest binding free energy (ΔG = -8.45 kcal/mol). This configuration included conventional hydrogen bonds with Arg90 (2.81 Å), Arg86 (2.17 Å), and Glu82 (2.74 Å), along with van der Waals interactions and electrostatic coordination near the Ca-3 coordinating residue, Asp93. Conversely, myricetin, kaempferol, and quercetin interacted primarily via van der Waals forces and hydrophobic contacts with residues surrounding the Asp93 locus (Phe89, Gly96, Gly98, and Tyr138), yielding higher binding free energies ranging from -7.18 to -6.82 kcal/mol (Figure 1, Table 5).

In the second grid, which encompassed multiple coordination spaces, rutin and quercetin engaged with both the first (Ca-1) and second (Ca-2) calcium-binding domains. Rutin (ΔG = -8.23 kcal/mol) formed hydrogen bonds with Thr26 (1.74 Å), Asp24 (2.76 Å), and Thr62 (2.17 Å), anchoring it near the Asp22, Glu31 (Ca-1), and Asn60 (Ca-2) residues. Quercetin (ΔG = -6.18 kcal/mol) established hydrogen bonds with Thr26, Asp24, Thr62, and Thr28 (distances: 2.15–3.60 Å) within the same functional domains (Figure 2). Myricetin and kaempferol displayed binding affinity scores of -4.42 and -4.02 kcal/mol, respectively, characterized by polar contacts with Asn60 or Thr28 and electrostatic interactions with Asp24.

Overall, all evaluated ligands interacted with residues from at least one calcium-binding domain (Ca-1, Ca-2, or Ca-3) encapsulated within the simulation search spaces. Figures 1 and 2 utilize individual panels to display primary coordinating residues, where spatial relationships are defined by atomic distance lines (Å) and the fourth calcium-binding domain (Ca-4) remains outside the active simulation coordinates.

DISCUSSION

Pharmacokinetic test

Pharmacokinetic evaluation via SwissADME assessed drug-likeness based on Lipinski's Rule of Five thresholds: molecular weight ≤500 g/mol, log P ≤5, no more than 5 hydrogen bond donors, no more than 10 hydrogen bond acceptors, and a molar refractivity between 40–130 cm^3/mol (Daina *et al.*, 2017; Lipinski *et al.*, 2001). Quercetin, kaempferol, and myricetin adhered to the MW and molar refractivity criteria, projecting bioavailability and membrane permeability (Lipinski *et al.*, 2001; Udoikono *et al.*, 2022). Furthermore, the evaluated compounds exhibited negative log P values below 5, individual scores ranging from -0.56 for quercetin to -3.89 for rutin, suggesting a

calculated lipophilicity-hydrophilicity profile that facilitates distribution within biological systems and interaction with intracellular targets like calmodulin (Tang *et al*., 2023).

While quercetin and kaempferol complied with H-bond limits, myricetin (6 donors) and rutin (10 donors, 16 acceptors) exceeded the thresholds. Rutin further deviated with a MW of 610.52 g/mol and molar refractivity of 141.38 cm^3/mol, theoretically limiting its passive cellular penetration. However, drug-likeness parameters are guidelines rather than rigid constraints, especially for complex natural compounds (Karami *et al*., 2022; Flores-Holguín *et al*., 2021).

Despite these violations, rutin was retained for subsequent simulations due to its bioactivity documented in previous literature (Nnemolisa *et al*., 2024; Pentu *et al*., 2025; Singh *et al*., 2024). Since Lipinski's rules primarily predict oral absorption, rutin's potential application is directed toward non-oral frameworks. Pharmacokinetic data indicates that oral rutin is metabolized to quercetin glucuronides/sulfates, leaving the parent compound undetectable in the bloodstream (Yang *et al*., 2005). To directly target calmodulin, intravenous administration of rutin nanoliposomes represents a future formulation strategy to optimize tissue delivery (Han *et al*., 2026). While direct tissue-level binding via this route requires further confirmation, rutin has demonstrated calcium/calmodulin-dependent protein kinase II (CaMKII) activation in skeletal muscle *in vivo* (Kappel *et al*., 2013), indicating pathway engagement. This *in silico* screening serves as a preliminary indicator, justifying further *in vitro* and *in vivo* validation.

Toxicity test

Toxicity evaluation via ProTox categorized the flavonoids based on the Globally Harmonized System (GHS), where lower LD_{50} values signify higher acute toxicity (Nursanti *et al*., 2022; Drwal *et al*., 2014; Graham *et al*., 2021). Quercetin and myricetin (LD_{50} = 159 mg/kg) were assigned to Class 3, predicting moderate toxicity in dose formulation. This computational prediction for quercetin aligns with rodent data, which reports oral LD50 values of 161 mg/kg for rats and 159 mg/kg for mice (Chang *et al*., 2021). While quercetin is consumed safely in dietary contexts via low-dose chronic ingestion, the ProTox-II prediction captures acute, high-dose risk driven by localized toxicophore fragment matching. This reactivity is likely linked to hydroxyl groups at the 3- and 5-positions, which enhance electron donation and potential metabolite toxicity (Jan *et al*., 2022). Conversely, kaempferol and rutin (LD50 = 3919 and 5000 mg/kg) fell into Class 5, indicating a lower acute toxicity profile. Rutin's lower toxicity profile is consistent with its glycosylated structure, which exhibits reduced cytotoxicity compared to its aglycone counterparts (Choi *et al*., 2021).

Although quercetin and myricetin exhibit higher acute toxicity, a low LD_{50} does not eliminate therapeutic viability, as evidenced by established drugs like warfarin or high-dose aspirin that require strict therapeutic windows (Noga *et al*., 2023; Habet, 2021). The limitations of moderate toxicity and bioavailability are currently addressed through advanced delivery systems and precision medicine strategies (Safe *et al*., 2021). Given that *in silico* predictions are preliminary estimations, the compounds remain candidates for further *in vitro* and *in vivo* validation to confirm safety and efficacy profiles.

Biological activity test

Biological activity was predicted based on Structure–Activity Relationship (SAR) principles to estimate the antioxidant potential of the flavonoids (Filimonov *et al*., 2014). In the PASS Online model, a Pa value > 0.7 serves as a statistical probability indicator of activity in experimental settings rather than an absolute certainty, reflecting a cross-validation accuracy that exceeds 85% to 90% for antioxidant mechanisms (Shamsuddin *et al*., 2021; Jairajpuri *et al*., 2021; Fakih *et al*., 2022).

Myricetin (0.924), rutin (0.923), quercetin (0.872), and kaempferol (0.856) yielded Pa values exceeding the Pi threshold of 0.003. Since all scores surpassed the 0.7 benchmark, these compounds are projected to possess a high probability of antioxidant activity, with myricetin showing the initial score (Basha *et al*., 2018). These results support their selection for target-specific interaction analysis, enabling strategic prioritization before laboratory validation.

Molecular docking

Molecular docking results demonstrated that all tested compounds interacted with the Calmodulin–Ca^{2+} receptor at two different binding areas (Grid 1 and Grid 2). The binding energy of a ligand–receptor complex is influenced by various intermolecular interactions, including hydrogen bonds, hydrophobic contacts, and electrostatic forces. Ligand conformations that complement the receptor binding site produce negative ΔG values, indicating stable interactions. Additionally, ligands with conformational flexibility adapt to the receptor, altering binding affinity (Tallei *et al*., 2023). However, flexible ligands like rutin risk producing false positives in traditional simulations. To address this, the Gnina docking engine utilizes a convolutional neural network (CNN) empirical scoring function that applies structural penalties for conformational entropy loss and steric clashes, ensuring that low ΔG scores reflect localized interaction specificity rather than random

conformational artifacts.

In this study, four flavonoid ligands, specifically quercetin, myricetin, rutin, and kaempferol, were evaluated for their molecular interactions with the calmodulin–Ca^{2+} complex using docking simulations. All tested ligands produced negative ΔG values (<0), indicating binding affinities toward the target protein, consistent with the principle that lower ΔG values reflect stable ligand–receptor complexes (Pebriana *et al*., 2012).

Among the compounds, rutin exhibited the most negative binding free energies across both docking regions, with ΔG values of −8.45 kcal/mol in the first grid box and −8.23 kcal/mol in the second, indicating the strongest predicted affinity for the calmodulin–Ca^{2+} complex. In the first grid box, myricetin ranked second (−7.18 kcal/mol), followed by kaempferol (−6.92 kcal/mol) and quercetin (−6.82 kcal/mol). In the second grid box, quercetin showed improved affinity (−6.18 kcal/mol), followed by myricetin (−4.42 kcal/mol) and kaempferol (−4.02 kcal/mol). This mid-range binding free energy for quercetin across both spaces suggests that calmodulin functions as a plausible physiological target rather than an irreversible inhibitor, a profile highly relevant for signaling sensors to permit dynamic, competitive modulation of calcium pathways. These computed energy ranges mathematically estimate low-micromolar to high-nanomolar dissociation constants (Kd), matching post-dietary plasma concentration thresholds for functional target engagement.

Structural modifications such as methylation, hydroxylation, and glycosylation influence the absorption, metabolic fate, and biological activities of flavonoids *in vivo*. Previous findings have shown that glycosylation and hydrogenation of the C2=C3 double bond alter the binding affinity of flavonoids for xanthine oxidase (Yuan *et al*., 2019), suggesting that similar modifications affect interactions with other target proteins, including calmodulin Ca^{2+}. While direct comparative binding benchmarks for these specific structures are limited, independent biological data supports rutin's functional interaction with calmodulin-dependent signaling; rutin has been documented to promote adipose tissue browning partially through the calmodulin-dependent protein kinase kinase β/AMP-activated protein kinase (CaMKKβ/AMPK) pathway (Ma *et al*., 2022). These findings, obtained through docking analysis with Gnina, suggest that rutin has a stable interaction configuration with the calcium-bound calmodulin complex, supporting its potential role in modulating calcium ion activity through complex formation.

Visualization

Visualization analysis identified the amino acid residues involved in ligand–receptor binding, which form contacts that contribute to inhibitory activity (Sari *et al*., 2020). By comparing flavonoid structures, the nature and strength of their biological interactions were elucidated. Types of interaction evaluated included hydrogen bonds, hydrophobic contacts, electrostatic forces, and interatomic distances (Prasetiawati *et al*., 2021).

Hydrogen bonds were represented by dark green dashed lines corresponding to specific residues. These bonds facilitate precise interactions between ligand hydrogen atoms and receptor residues, which stabilize molecular conformations and enhance binding specificity. Electrostatic interactions, which are non-covalent forces between oppositely charged regions, further contribute to the positioning of ligands within the binding pocket (de Freitas and Schapira, 2017).

To interpret the docking interactions, it is essential to consider the dynamic architecture of calmodulin, particularly its EF-hand domains and flexible linker. These structural features contribute to calmodulin's ability to undergo conformational changes upon Ca^{2+} binding, which influence ligand accessibility and binding affinity at different sites. In the docking simulations using two distinct grid box areas targeting different Ca^{2+} binding regions, each ligand exhibited unique interaction patterns and ΔG values. Although the docking data provides numerical outcomes, the visualization highlights why rutin consistently showed the lowest ΔG: it formed multiple hydrogen bonds and hydrophobic contacts with key residues in the binding pocket, specifically establishing directional polar clusters with Arg90, Arg86, and Glu82 to suggest localized specificity rather than generic hydrophobic partitioning.

These observations can be linked to the structural characteristics of each compound. Certain flavonoid structures tend to form intramolecular hydrogen bonds, reducing planarity and limiting the availability of hydrogen donors for intermolecular bonding with protein residues (Spiegel *et al*., 2020). Furthermore, interactions between flavonoids and their targets are driven by hydrogen bonding and contacts when polar functional groups are positioned (Priani and Fakih, 2021). Although that study focused on citrus peel flavonoids, the interaction trends remain consistent across different flavonoid classes, including those from *Syzygium cumini*, suggesting a common mechanism underlying ligand–protein affinity.

In contrast, other ligands had fewer interactions, reflecting their higher ΔG values. Thus, the orientation and availability of polar groups among the tested flavonoids explain the variations in their interaction types and binding energies, with rutin exhibiting a structurally favorable profile for

interaction with calmodulin-Ca^{2+}.

Based on the *in silico* analysis, flavonoid compounds from *Syzygium cumini*, namely quercetin, myricetin, rutin, and kaempferol, are predicted to interact with Ca^{2+} through binding to calmodulin protein, involving hydrogen bonds, hydrophobic interactions, and electrostatic forces. Among them, rutin exhibited the lowest ΔG, with values of −8.45 kcal/mol in the first docking region and −8.23 kcal/mol in the second, indicating stable interaction with the calcium-bound calmodulin. These findings suggest that rutin may serve as a structural hit configuration among the tested flavonoids for future evaluation in modulating calcium signaling through calmodulin-binding.

Study limitations

This screening is subject to several screening constraints inherent to structural modeling tools. First, the binding models operate as computational point estimates without empirical wet-lab validation via quantitative biophysical assays. Second, the docking simulations used a static, rigid crystal conformation of calmodulin (PDB ID: 1CLL), which excludes structural flexibility and dynamic loop movements. Third, the localized interaction scoring applied implicit solvation models, omitting the dynamic water network configurations that influence physiological thermodynamic bindings over time.

CONCLUSIONS

This computational screening indicates that flavonoid compounds from *Syzygium cumini* possess structural compatibility to interact with the calcium-bound calmodulin receptor. The data do not demonstrate direct functional modulation of cellular signaling loops. Within this comparative framework, rutin exhibited binding free energies of -8.45 kcal/mol and -8.23 kcal/mol across separate search regions. The single primary conclusion is that rutin serves as the base structural template among the evaluated compounds due to these lower energy metrics. These computational findings are preliminary, and direct experimental validation is required before any therapeutic applications can be evaluated.

To maintain an objective framework, several methodological characteristics of this initial virtual screening should be noted. First, the generated binding free energies operate as deterministic point estimates derived under a fixed random seed constraint (-seed 0) to secure exact reproducibility, which inherently excludes random algorithmic variance. Second, this initial profiling focuses on the relative comparative performance among the native phytochemical constituents of *S. cumini* without incorporating exogenous reference inhibitors. Third, the structural fragment mapping utilized in the activity screening reflects the resolution boundaries of the baseline training library. Finally, the structural attributes of rutin predict restricted passive oral absorption, meaning its physiological relevance is linked to non-oral delivery systems or advanced nanoliposomal formulations rather than standard oral delivery.

To transition these virtual screening metrics into empirical validation, targeted biophysical testing is required. Surface Plasmon Resonance (SPR) assays will be prioritized to directly quantify the binding kinetics between rutin and immobilized calmodulin-Ca^{2+} complexes. The extraction of a dose-dependent sensorgram demonstrating a specific equilibrium dissociation constant (Kd) within the low-micromolar to high-nanomolar range will confirm the binding affinities estimated by the docking model, whereas the observation of a non-specific or flat binding profile across expanding concentrations will mathematically refute the computational hypothesis.

ACKNOWLEDGMENTS

The authors express their sincere gratitude to the Faculty of Veterinary Medicine, Universitas Airlangga, for the support and facilities provided throughout this *in silico* research. This study did not involve any funding.

NOVELTY STATEMENT

This study presents a new application of established computational tools by evaluating the structural interactions of *Syzygium cumini* flavonoids with the calmodulin-Ca^{2+} complex. The findings characterize the predicted binding affinity and safety profiles of these compounds, offering baseline structural configurations for future evaluation.

AUTHOR'S CONTRIBUTION

Conceptualization, data analysis, molecular docking simulations, visualization analysis, interpretation of interaction profiles and writing original draft: NDNC. Methodology: NDNC, LM. Supervision: LM, R. Validation: NDNC, LM, R, KR, RD, MS. Writing review and editing: NDNC, LM, R, KR, RD, MS.

Generative AI and AI assisted technology statement

The authors used artificial intelligence-based tools solely for language polishing and grammar improvement. No AI tools were used in data analysis, interpretation, or the creation of scientific content. All results and interpretations were conducted and verified by the authors.

Conflict of interest

The authors have declared no conflict of interest.

REFERENCES

Basha SAA, Yunoos M, Ahmed J (2018). PASS: A Computerized Prediction of Biological Activity Spectra for Chemical Substances. Indo Am. J. Pharm. Res., 8(6): 1442.

Bertero E, Maack C (2018). Calcium signaling and reactive oxygen species in Mitochondria. Circ. Res., 122(10): 1460-1478. https://doi.org/10.1161/CIRCRESAHA.118.310082

Chang SN, Kim HJ, Kang SC (2021). Quercetin mitigates oxidative stress, developmental toxicity and teratogenic effects induced by high-dose vitamin D2 in Zebrafish Embryos. Turk. J. Fish. Aquat. Sci., 22(3). https://doi.org/10.4194/TRJFAS20269

Chattopadhyaya R, Meador WE, Means AR, Quiocho FA (1992). Calmodulin structure refined at 1.7 Å resolution. J. Mol. Biol., 228(4): 1177-1192. https://doi.org/10.1016/0022-2836(92)90324-D

Choi S-S, Park H-R, Lee K-AA (2021). Comparative study of rutin and rutin glycoside: Antioxidant activity, anti-inflammatory effect, effect on platelet aggregation and blood coagulation. Antioxidants, 10(11): 1. https://doi.org/10.3390/antiox10111696

Daina A, Michielin O, Zoete V (2017). Swiss ADME: A free web tool to evaluate pharmacokinetics, drug-likeness and medicinal chemistry friendliness of small molecules. Sci. Rep., pp. 1-10. https://doi.org/10.1038/srep42717

de Freitas RF, Schapira M (2017). A systematic analysis of atomic protein-ligand interactions in the PDB. Med. Chem. Commun., 8: 1970-1981. https://doi.org/10.1039/C7MD00381A

de Nicolo B, Cataldi-Stagetti E, Diquigiovanni C, Bonora E (2023). Calcium and reactive oxygen species signaling interplays in cardiac physiology and pathologies. Antioxidants, 12: 1-19. https://doi.org/10.3390/antiox12020353

Drwal MN, Banerjee P, Dunkel M, Wettig MR, Preissner R (2014). ProTox: A web server for the *in silico* prediction of rodent oral toxicity. Nucl. Acids Res., 42: W54-W55. https://doi.org/10.1093/nar/gku401

Fakih TM, Jannati FA, Meilani A, Ramadhan DSF, Darusman F (2022). Studi *in silico* aktivitas analog senyawa zizyphine dari bidara arab (*Zizyphus spina-christi*) sebagai Antivirus SARS-CoV-2 terhadap Reseptor 3CLpro). Al-Chemy J. Penelit. Kim., 18(1): 70-79. https://doi.org/10.20961/alchemy.18.1.52188.70-79

Filimonov DA, Lagunin AA, Gloriozova TA, Rudik AV, Druzhilovskii DS, Pogodin PV, Poroikov VV (2014). Prediction of The biological activity spectra of organic compounds using the pass online web resource. Chem. Heterocycl. Comp., 50(3): 444-457. https://doi.org/10.1007/s10593-014-1496-1

Flores-Holguín N, Frau J, Glossman-Mitnik D (2021). *In silico* pharmacokinetics, ADMET study and conceptual DFT analysis of two plant cyclopeptides isolated from rosaceae as a computational peptidology approach. Front. Chem., 9: 2-5. https://doi.org/10.3389/fchem.2021.708364

Giorgi C, Marchi S, Pinton P (2018). The machineries, regulation and cellular functions of mitochondrial calcium. Nat. Rev. Mol. Cell. Biol., 19(11): 713-730. https://doi.org/10.1038/s41580-018-0052-8

Graham JC, Rodas M, Hillegass J, Schulze G (2021). The performance, reliability and potential application of in silico models for predicting the acute oral toxicity of pharmaceutical compounds. Regul. Toxicol. Pharmacol., 119: 104816. https://doi.org/10.1016/j.yrtph.2020.104816

Guedes BN, De Oliveira Neto JG, Zielińska A, Santini A, Andreani T, Oliveira MBPP, Fathi F, Souto EB (2026). Polyphenols-composed micelles: Production, physicochemical characterization, *in silico* pharmacokinetics, and rheological behaviour of a new colloidal system for dual delivery of resveratrol and rutin. Pharm. Dev. Technol., 31(3): 413–427. https://doi.org/10.1080/10837450.2026.2624733

Gupta P, Khan S, Fakhar Z, Hussain A, Rehman MT, Al Ajmi MF, Islam A, Ahmad F, Hassan MI (2020). Identification of potential inhibitors of calcium/calmodulin-dependent protein kinase IV from bioactive phytoconstituents. Oxid. Med. Cell. Longev., 2020(1): 2094635. https://doi.org/10.1155/2020/2094635

Habet S (2021). Narrow therapeutic index drugs: Clinical pharmacology perspective. J. Pharm. Pharmacol., 73: 1285-1291. https://doi.org/10.1093/jpp/rgab102

Han JY, Liu YD, Ding H, Pang YH, Shen XF (2026). Fucoidan/chitosan coated nanoliposomes enhancing URAT1 targeting of rutin for alleviating hyperuricemia. Int. J. Biol. Macromol., 335: 149263. https://doi.org/10.1016/j.ijbiomac.2025.149263

Hempel N, Trebak M (2017). Crosstalk between calcium and reactive oxygen species signaling in cancer. Cell Calcium, 63: 70-96. https://doi.org/10.1016/j.ceca.2017.01.007

Hidayah H, Aziz A, Sevianti E, Noordiansyah MA (2023). Literature review: Jamblang (*Syzygium cumini* (L): A review of its bark and medicinal uses. J. Ilm Wahana Pendidik, 9(15): 193-199.

Jairajpuri DS, Hussain A, Nasreen K, Mohammad T, Anjum F, Rehman MT, Hasan GM, Alajmi MF, Hassan MI (2021). Identification of natural compounds as potent inhibitors of SARS-CoV-2 main protease using combined docking and molecular dynamics simulations. Saudi J. Biol. Sci., 28(4): 2423-2431. https://doi.org/10.1016/j.sjbs.2021.01.040

Jan R, Khan M, Asaf S, Lubna, Asif S, Kim K-M (2022). Bioactivity and therapeutic potential of kaempferol and quercetin: New insights for plant and human health. Plants, 11: 1-5. https://doi.org/10.3390/plants11192623

Kappel VD, Zanatta L, Postal BG, Silva FRMB (2013). Rutin potentiates calcium uptake via voltage-dependent calcium channel associated with stimulation of glucose uptake in skeletal muscle. Arch Biochem. Biophys., 532(2): 55-60. https://doi.org/10.1016/j.abb.2013.01.008

Karami TK, Hailu S, Feng S, Graham R, Gukasyan HJ (2022). Eyes on Lipinski's rule of five: A new rule of thumb for physicochemical design space of ophthalmic drugs. J. Ocul. Pharmacol. Ther., 38(1): 43. https://doi.org/10.1089/jop.2021.0069

Kumar M, Hasan M, Lorenzo JM, Dhumal S, Nishad J, Rais N, Verma A, Changan S, Barbhai MD, Radha, Chandran D, Pandiselvam R, Senapathy M, Dey A, Pradhan PC, Mohankumar P, Deshmukh VP, Amarowicz R, Mekhemar M, Zhang, B (2022). Jamun (*Syzygium cumini* (L.) Skeels) seed bioactives and its biological activities: A review. Food Biosci., 50: 102109. https://doi.org/10.1016/j.fbio.2022.102109

Lipinski CA, Lombardo F, Dominy BW, Feeney PJ (2001). Experimental and computational approaches to estimate solubility and permeability in drug discovery and development settings. Adv. Drug. Deliv. Rev., 46(1-3): 3-26. https://doi.org/10.1016/S0169-409X(96)00423-1

Ma B, Hao J, Xu H, Liu L, Wang W, Chen S, Wu H (2022). Rutin promotes white adipose tissue "browning" and brown adipose tissue activation partially through the calmodulin-dependent protein kinase kinase β/AMP-activated protein kinase pathway. Endocr. J., 69(4): 385-397. https://doi.org/10.1507/endocrj.EJ21-0441

Manach C, Morand C, Crespy V, Demigné C, Texier O, Régérat F, Rémésy C (1998). Quercetin is recovered in human plasma as conjugated derivatives which retain antioxidant properties. FEBS Lett., 426(3): 331-336. https://doi.org/10.1016/S0014-5793(98)00367-6

Millana Fañanás E, Todesca S, Sicorello A, Masino L, Pompach P, Magnani F, Pastore A, Mattevi A (2020). On the mechanism of calcium-dependent activation of NADPH oxidase 5 (NOX5). FEBS J., 287(12): 2486-2503. https://doi.org/10.1111/febs.15160

Munteanu IG, Apetrei C (2021). Analytical methods used in determining antioxidant activity: A review. Int. J. Mol. Sci., 22: 1-30. https://doi.org/10.3390/ijms22073380

Nnemolisa SC, Chukwurah CC, Edeh SC, Aguchem RN, Chibuogwu CC, Aham EC, Chukwu MC, Obiora MO, Anyebe DE, Okagu IU (2024). Antidiabetic and antioxidant potentials of Pleurotus ostreatus-derived compounds: An *in vitro* and *in silico* approach. Food Chem. Adv., 4: 1-8. https://doi.org/10.1016/j.focha.2024.100639

Noga M, Michalska A, Jurowski K (2023). Application of toxicology *in silico* methods for prediction of acute toxicity (LD_{50}) for Novichoks. Arch. Toxicol., 97: 1691-1700. https://doi.org/10.1007/s00204-023-03507-2

Nursanti O, Aziz A, Hadisoebroto G (2022). Docking dan uji toksisitas secara insilico untuk mendapatkan kandidat obat analgesik. Inpharnmed, 6(1): 35-46. https://doi.org/10.21927/inpharnmed.v6i1.1922

Ontiveros M, Rinaldi D, Marder M, Espelt MV, Mangialavori I, Vigil M, Rossi JP, Ferreira-Gomes M (2019). Natural flavonoids inhibit the plasma membrane Ca2+-ATPase. Biochem. Pharmacol., 166: 1-11. https://doi.org/10.1016/j.bcp.2019.05.004

Paliyath G, Poovaiah BW (1985). Identification of naturally occurring calmodulin inhibitors in plants and their effects on calcium-and calmodulin-promoted protein phosphorylation. Plant Cell Physiol., 26(1): 201-209. https://doi.org/10.1093/oxfordjournals.pcp.a077017

Pebriana RB, Romadhon AF, Yunianto A, Rokhman MR, Fitriyah NQ, Jenie RI, Meiyanto E (2012). Docking Kurkumin dan Senyawa Analognya Pada Reseptor Progesteron: Studi Interaksinya Sebagai Selective Progesterone Receptor Modulators (SPRMs). Pharmacon, 13(2): 55-60. https://doi.org/10.23917/pharmacon.v13i2.10

Pentu N, Azhakesan A, Kumar PK (2025). *In silico* molecular docking and ADME/T studies of flavonol compounds against selected proteins involved in inflammation mechanism. J. Appl. Pharm. Res., 13(1): 95-111. https://doi.org/10.69857/joapr.v13i1.706

Pepke S, Kinzer-Ursem T, Mihalas S, Kennedy MB (2010). A Dynamic Model of Interactions of Ca2+ , Calmodulin, and Catalytic Subunits of Ca2+ /Calmodulin-Dependent Protein Kinase II. PLoS Comput. Biol., 6(2): 1-3. https://doi.org/10.1371/journal.pcbi.1000675

Picq M, Dubois M, Prigent AF, Nemoz G, Pacheco H (1989). Inhibition of the different cyclic nucleotide phosphodiesterase isoforms separated from rat brain by flavonoid compounds. Biochem. Int., 18(1): 47-57.

Prasetiawati R, Suherman M, Permana B (2021). Molecular docking study of anthocyanidin compounds against epidermal growth factor receptor (EGFR) as anti-lung cancer. Indones. J. Pharm Sci. Technol., 8(1): 8-20. https://doi.org/10.24198/ijpst.v8i1.29872

Priani SE, Fakih M (2021). Insights into molecular interaction of flavonoid compounds in citrus peel bound to collagenase and elastase enzymes: A computational study. Pharm. Sci. Res., 8(2): 93-101. https://doi.org/10.7454/psr.v8i2.1202

Safe S, Jayaraman A, Chapkin RS, Howard M, Mohankumar K, Shrestha R (2021). Flavonoids: structure–function and mechanisms of action and opportunities for drug development. Toxicol. Res., 37: 147. https://doi.org/10.1007/s43188-020-00080-z

Sakurada R, Odagiri K, Hakamata A, Kamiya C, Wei J, Watanabe H (2019). Calcium release from endoplasmic reticulum involves calmodulin-mediated NADPH oxidase-derived reactive oxygen species production in endothelial cells. Int. J. Mol. Sci., 20(7): 1644. https://doi.org/10.3390/ijms20071644

Sari IW, Junaidin, Pratiwi D (2020). Studi Molecular Docking Senyawa Flavonoid Herba Kumis Kucing (*Orthosiphon stamineus* B.) Pada Reseptor. Glucosidase Sebagai Antidiabetes Tipe 2. J. Farmagazine, 7(2): 54-60. https://doi.org/10.47653/farm.v7i2.194

Shaker B, Ahmad S, Lee J, Jung C, Na D (2021). *In silico* methods and tools for drug discovery. Comput. Biol. Med., 137: 1-10. https://doi.org/10.1016/j.compbiomed.2021.104851.

Shamsuddin T, Hosen MA, Alam MS, Emran TB, Kawsar SMA (2021). Uridine derivatives: Antifungal, PASS outcomes, ADME/T, drug-likeliness, molecular docking and binding energy calculations. Med. Sci., 10(4): 1374. https://doi.org/10.5455/medscience.2021.05.175

Singh S, Kumar S, Dhanasingh I (2024). *In-silico* identification of flavonoids based inhibitors against sortase-A from *Enterococcus faecalis (Ef)*. J. Microbiol. Biotechnol. Food Sci., 14(2): 1-5. https://doi.org/10.55251/jmbfs.11256

Spencer JPE, Abd El-Mohsen MM, Minihane A-M, Mathers JC (2008). Biomarkers of the intake of dietary polyphenols: strengths, limitations and application in nutrition research. Br. J. Nutr., 99(1): 12-22. https://doi.org/10.1017/S0007114507798938

Spiegel M, Andruniów T, Sroka Z (2020). Flavones and flavonols antiradical structure–activity relationship: A quantum chemical study. Antioxidants, 9(6): 1-22. https://doi.org/10.3390/antiox9060461

Tallei TE, Fatimawali, Adam AA, Ekatanti D, Celik I, Fatriani R, Nainu F, Kusuma WA, Rabaan AA, Idroes R (2023). Molecular insights into the anti-inflamatory activity of fermented pineapple juice using multimodal computational studies. Arch. Pharm. (Weinheim), 357(1): 2300422. https://doi.org/10.1002/ardp.202300422

Tang Q, Tan P, Dai Z, Wang T, Xu S, Ding Y, Jin J, Zhang X, Zhang Y, Zhou C, Yue Z, Huiyang F, Yan J, Ma X (2023). Hydrophobic modification improves the delivery of cell-penetrating peptides to eliminate intracellular pathogens in animals. Acta Biomater., 157: 210-224. https://doi.org/10.1016/j.actbio.2022.11.055

Tessema FB, Gonfa YH, Asfaw TB, Tadesse MG, Bachheti RK (2023). Antioxidant activity of flavonoids and phenolic acids from Dodonaea angustifolia flower: HPLC profile and PASS prediction. J. Chem., 2023(1): 8315711. https://doi.org/10.1155/2023/8315711

Tirone F, Cox JA (2007). NADPH oxidase 5 (NOX5) interacts with and is regulated by calmodulin. FEBS Lett., 581(6): 1202-1208. https://doi.org/10.1016/j.febslet.2007.02.047

Udoikono AD, Louis H, Eno EA, Agwamba EC, Unimuke TO, Igbalagh AT, Edet HO, Odey JO, Adeyinka AS (2022). Reactive azo compounds as a potential chemotherapy drugs in the treatment of malignant glioblastoma (GBM): Experimental and theoretical studies. J. Photochem. Photobiol., 10: 1-25. https://doi.org/10.1016/j.jpap.2022.100116

Yang CY, Hsiu SL, Wen KC, Lin SP, Tsai SY, Hou YC, Chao PD (2005). Bioavailability and metabolic pharmacokinetics of rutin and quercetin in rats. J. Food Drug Anal., 13(3): 5. https://doi.org/10.38212/2224-6614.2517

Yuan M, Liu Y, Xiao A, Leng J, Liao L, Ma L, Liu L (2019). The interaction of dietary flavonoids with xanthine oxidase *in vitro*: molecular property-binding affinity relationship aspects. RSC Adv., 9: 10781-10788. https://doi.org/10.1039/C8RA09926J